On-chip optical nano-scale displacement sensor

Peng Wang, Aron Michael, Chee Yee Kwok;
The University of New South Wales

ABSTRACT

In this paper, a high-speed on-chip optical displacement sensing and self-actuating mechanisms have been designed and simulated for an AFM application. This mechanism can allow significantly smaller cantilever beams to be made with higher sensitivity and wide bandwidth for parallel imaging through array of cantilevers. This arrangement consists of a Si-waveguide in which a nano-scale free space gap is fabricated in the direction of light propagation. One portion of the Si-waveguide is a suspended cantilever with a thin film PZT formed on it for actuation. The optical power coupling loss between the waveguides is used to measure the cantilever displacement. The simulation results show that the device can achieve a 6.25MHz resonant frequency in air, 0.195N/m spring constant and less than 0.1nm sensitivity. This approach can overcome the conventional cantilever size limit of an AFM to achieve high bandwidth with low spring constant.

Keywords: On-chip, nano-scale, optical, sensor, high-speed, self-actuating.

1.2 INTRODUCTION

Atomic Force microscopy (AFM) was invented by Bining and Rohrer in 1986[1], and decades later it became widely used as a nanometer scale topology scanner in many fields. In AFM, a micro-cantilever with a sharp tip at the free end plays an essential role in the imaging mechanism. The nanoscale tip-sample interaction leads to the deflection of the cantilever, which is optically detected. The interaction portion is varied over the imaging area of the sample by the XY-scanning of the sample stage while Z-scanning, based on the feedback control system, provides surface topology information of the object under investigation.

Unlike traditional microscopy, AFM has the ability to capture 3D-images of objects in both air and liquid environment with high resolution[2]. This capability has been used to observe the structure and the activities of many bio-molecular processes in biological sciences[3]. However, the low imaging rate of conventional AFM has limited its application in dynamic biological system. Over the past decade, researchers have been investigating various techniques to increase the scanning speed of AFM. A high speed AFM that can capture image at 25 frames per second with scan range of $240 \times 240\ nm^2$ and 100 scan lines has been designed by T.Ando[4]. Although, the dynamic bimolecular process can be captured on video successfully, it can only be achieved in a very small area and certain molecular process still could not be resolved. Thus, high speed AFM continues to be a subject of intensive investigation.

One of the major critical issues that limit the operating speed of Scanning Probe Microscopy is the relatively large size of the micro-cantilever. As the cantilever size is reduced the resonance frequency increases, thereby allowing higher imaging rate. In addition to increasing the resonance frequency, the design of the micro-cantilever should also have a small spring constant so as to reduce the tip force acting on the sample. Although these two conflicting requirements are not easy to achieve, reducing the size of the cantilever is a necessary procedure. However, the current size of the cantilever is limited by the optical beam spot size dimension which is required by the Optical Beam Deflection (OBD) detection system. Hence, to solve this problem, a new detection mechanism is necessary.

*peng.wang3@student.unsw.edu.au; phone 61 450 259888

Micro/Nano Materials, Devices, and Systems, edited by James Friend, H. Hoe Tan, Proc. of SPIE
Vol. 8923, 89233Z · © 2013 SPIE · CCC code: 0277-786X/13/$18 · doi: 10.1117/12.2033715

In this paper, a self-sensing and actuation mechanism for AFM applications has been designed and simulated. After describing the proposed structure, theoretical and simulation studies on the structure will be presented in section 2. This new approach does not rely on the width of the cantilever beam and hence it overcomes the existing bottleneck. A piezoelectric film integrated on the cantilever allows self-actuation feature in the z-direction is covered in section3.

2. OPTICAL CANTILEVER DEFLECTION SENSING SYSTEM

2.1 Sensor structure

Figure 1(a) and (b) show the 3-D schematic diagram of the optical sensor system and the cross-sectional view along the A-A' direction, respectively. The sensor system consists of two silicon waveguides facing each other with a small (nano-scale) gap in between. The silicon waveguides are suspended as cantilever beams with the input silicon waveguides having PZT thin film integrated on top. Both waveguides have slanted grating at one end to allow optical beam coupling from vertical optical fibers. The whole structure can be fabricated on a silicon-on-insulator (SOI) wafer. The input and output optical fibers are inserted into the through-holes for coupling the optical beam to and from input and output silicon waveguides, respectively, via slanted gratings.

In the new sensor system, an optical beam is generated by a laser source and coupled to the input fiber. The gratings couple the beam to the input silicon cantilever waveguide, and then the beam is received by the output cantilever waveguide on the other side. The beam is coupled to the output fiber through the grating at the output end, and is then detected by a photodiode to measure the power loss. When the input waveguide moves in z direction, it will cause a change in detected power. Thus, the movement can be detected based on this power loss. This approach allows much smaller silicon cantilever beam with significantly reduced width to be made.

2.2 Sensor design

In order to achieve high sensitivity, the power loss per unit z-displacement is required to be as large as possible. Four major parameters affect the power loss: (i) cantilever thickness, (ii) offset, (iii) cantilever gap and (iv) silicon dioxide cladding thickness. In order to understand the effect of each of these parameters, we have carried out a number of FDTD simulations.

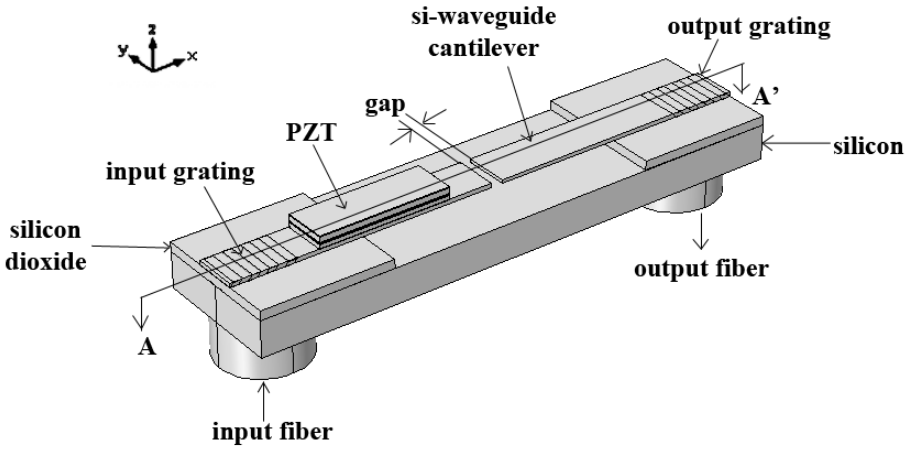

Figure 1(a). 3-D schematic diagram of the optical sensor system.

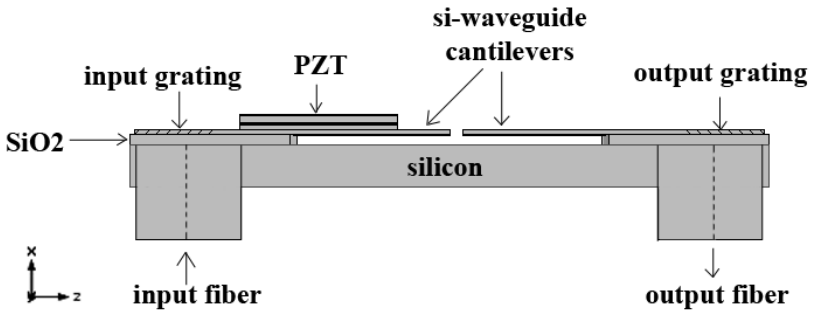

Figure 1(b). Cross-sectional view of the optical sensor system along the A-A' direction.

2.2.1 Cantilever thickness & offset

The new sensor must be designed such that the silicon waveguide operates in single mode. In order to maintain the single mode operation, the normalized frequency should be less than 2.405 and this requirement limits the maximum thickness of the waveguide. The minimum thickness of the waveguide (h_{min}), however, is determined by the cladding material. With a SiO_2 as cladding, h_{min} is given by[5]

$$h_{min} = \frac{0.5\lambda}{2({n_1}^2 - {n_2}^2))^{\frac{1}{2}}} \quad (1)$$

where λ, n_1 and n_2 represent the wavelength of the beam, the refractive index of silicon and the refractive index of SiO_2, respectively. Hence, the cantilever should have a thickness in the range $0.17um \leq h \leq 0.26um$.

The mode shape in the waveguide varies with different thicknesses of cantilever, which can impact on power loss per unit displacement. To find out the optimal cantilever thickness, four sets of simulations with different thickness (0.17um, 0.18um, 0.19um and 0.2um.) have been performed. The simulations are carried out using 2D-FDTD at 1.55um wavelength. Figure 2 shows the simulated structure. An offset between the input and output waveguide cantilevers is considered to take into account the z-direction displacement of the input silicon waveguide cantilever. The angular misalignment can be neglected, as the displacement in z-direction is much smaller than the length of the input silicon waveguide cantilever.

Figure 3 indicates the power loss per 5nm displacement for different thickness of cantilevers with varying offset between the input and output cantilever (the gap is 20nm). It shows that the power loss occurs at different offsets for various cantilever thickness. The maximum sensitivity is 2.152%/5nm for the cantilever thickness of 130nm at 140nm offset.

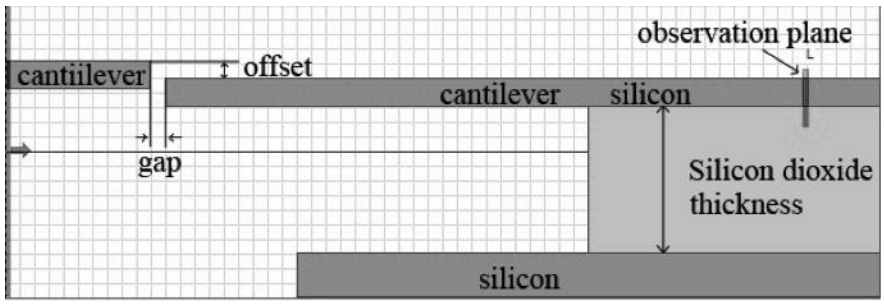

Figure 2. The sensor structure in OptiFDTD simulation.

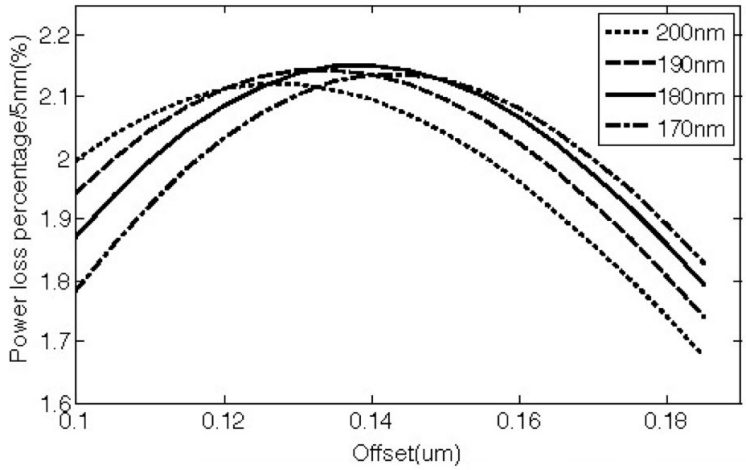

Figure 3. The percentage of power loss per 5nm with different cantilever thickness (20nm gap, and 0.31um observer. regardless of silicon dioxide cladding effect).

2.2.2 Gap between cantilevers

The gap between the two waveguides also affects the sensitivity. The sensitivity of the sensor for different gaps with 180nm cantilever (surrounded by air) thickness has been simulated and shown in Figure 4. The figure indicates that the smaller gap leads to a larger sensitivity, and the max sensitivity is 2.239%/5nm for 10nm gap.

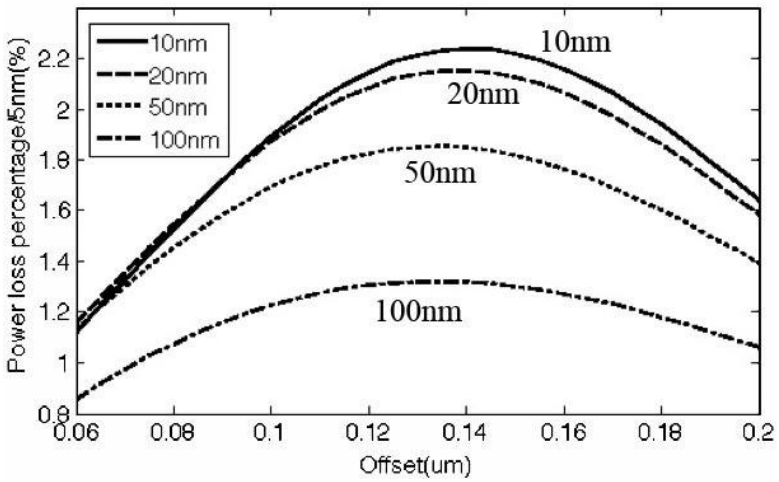

Figure 4. The percentage of power loss per 5nm for various gaps (180nm cantilever thickness, 0.31um observer and regardless of the silicon dioxide cladding effect).

Although the smaller gap provides larger power loss, the smallest gap that can be achieved is limited by the in-plane movement of the deflected cantilever albeit small. Otherwise the two waveguides may end up touching each other. The other factor that may limit the separation distance is the smallest gap that can be faithfully fabricated by the existing VLSI technology mode, which isn't better than 10nm. Thus, the 10nm gap has been chosen, as it provides relatively large sensitivities and is realizable.

2.2.3 SiO_2 thickness

In earlier simulations, all the waveguides were assumed to be surrounded by air. However, the waveguides will be fabricated on a SOI wafer with a SiO_2 layer underneath them. If the thickness of SiO_2 layer is too thin, some portion of the energy will be coupled to the silicon substrate, which will reduce sensitivity to power loss variations.

Figure 5 shows the sensitivities for different SiO_2 cladding thicknesses (cantilever thickness =180nm, and gap =10nm). We can see that the sensitivity is much lower than the previous air ambient if the SiO_2 layer is less than 0.2um thick. The reason is that a large portion of optical energy will be coupled to the silicon substrate. With the thicker SiO_2 cladding, the sensitivity increases until it reaches to the same value as the air ambient. Therefore, in order to get larger sensitivity at an offset of 140um, SiO_2 cladding thickness of more than 0.3um should be used.

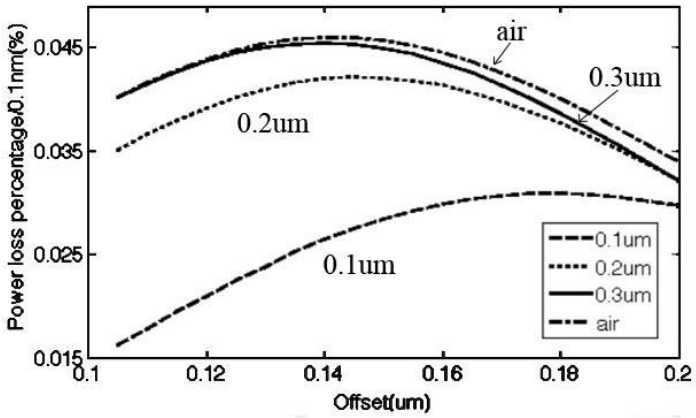

Figure 5. Power loss for different SiO_2 layer thicknesses (0.18um cantilever thickness, 10nm gap).

3. Piezoelectric Actuator

In order to allow self-actuating feature for the z-direction, a piezoelectric layer is deposited on the top of the input silicon waveguide in our design. Such arrangement can enable fast z-scanning and the use of a cantilever array for parallel imaging.

3.1 Piezoelectric material

Lead zirconate titanate (PZT) and zinc oxide (ZnO) are two common piezoelectric materials that can be considered as candidates. Typically, PZT has larger piezoelectric coefficient than ZnO, but ZnO is easier to fabricate. Both piezoelectric materials can be used as piezoelectric layer for the actuator. In our sensor system, relatively large scanning range is desired. Considering the electromechanical coupling coefficient and the break down voltage of the piezoelectric materials, PZT as an actuator material is chosen. In following simulation work, PZT-5A was used as the piezoelectric material.

3.2 Actuator structure

As shown in figure 1(a) and (b), the actuator consists of six layers, Pt, PZT, Pt, Ti, SiO_2 and Si. For the design purpose, the thickness of Pt, Ti, SiO_2 and Si are fixed while the dimension of PZT layer and the cantilever length are varied to maximize the resonance frequency and minimize the spring constant of the actuator. The design parameters and material constants and other relevant dimensions are provided in Table 1.

Table 1. Key data of the actuator.

Layer	w (um)	h (nm)	ρ (kg/m^3)	E(Gpa)
Si	0.2	180	2330	165
SiO_2	0.2	300	2200	70
Ti	0.2	10	4506	115.7
Pt (up)	0.2	60	21450	168
Pt (down)	0.2	60	21450	168
PZT	0.2	varied	7750	61

3.2.1 Cantilever z-displacement range

The cantilever z-displacement range extends between the minimum and maximum displacements. In practice, thin films will have residual stress and stress gradient, and in multi-layer structure, this may lead to residual moment and hence bending, which produces initial out-of-plane z-displacement. When a voltage is applied across the PZT layer, the cantilever moves in a positive z or negative z direction depending on the polarity of the voltage. When a voltage in the direction of polarization is applied, the cantilever moves in the positive z-direction. The displacement increases as the voltage increase. However, the maximum deflection is limited by the breakdown voltage. This voltage will determine the maximum positive z-displacement of the actuator. The displacement in the opposite direction is limited by the depolarizing voltage, which is usually in the range of 3-6V/um. This will set the minimum z-displacement.

The equation for the maximum electric field strength (E_{max}) for a known $Pb(Zr_{0.52}Ti_{0.48})O_3$ layer thickness (d) is given by Sergey et al. as[6]

$$E_{max} = \gamma d^{-w} \qquad (2)$$

where γ is a constant for PZT material, and w is a coefficient determined by the mechanisms of electric breakdown.

Based on the work of Sergey et al., a set of coefficients of $\gamma = 4.65$ and $w = 0.25$ can be used to calculated the breakdown voltages for 0.15, 0.25, 0.35um and 0.5um thick PZT layers, and they are about 6V, 9V, 12V and 15V, respectively.

Table 2 shows simulated out-of-plane displacements due to residual stresses in oxide and PZT thin films. A compressive stress of 300MPa for oxide and a tensile stress of 100MPa for PZT with a piezoelectric charge coefficient e_{33} of $15.7835 C/m^2$ are used in the simulation. These stress values are typical for these two thin films. The effect of residual stress in the other films can be neglected, as the film thicknesses are relatively thin. In addition to the initial out-of-plane displacements, the maximum achievable displacements are limited by the breakdown voltage of the PZT film used. It can be seen from the table that the out-of-plane displacement due to the residual stress and the maximum displacement achievable increases as the thickness of PZT increases until some value of PZT thickness is reached. Further increase in PZT thickness reduces the deflection. Therefore, there is an optimal PZT thickness that can be used to achieve the maximum deflection. Considering an effective operation range of 0 to 200nm and the initial deflection position of 140nm, 0.25um thick PZT layer and 12um long cantilever have been chosen.

Table 2. Minimum and maximum cantilever z-displacement for different PZT layer dimensions.

PZT length/cantilever length (um)	PZT layer thickness (um)	Initial displacement (nm)	Maximum displacement (nm)	Displacement range
5/12	0.15	12.7	155.2	142.5
8/12	0.15	32.2	208.2	176
5/12	0.25	37.6	202.3	164.7
8/12	0.25	65.7	275.9	210.2
5/12	0.35	49.2	220.8	171.6
8/12	0.35	82.8	307	224.2
5/12	0.5	54.1	205.2	151.1
8/12	0.5	91.6	294	202.4

3.2.2 Resonant frequency & spring constant

A cantilever with a high resonant frequency is essential for high-speed AFM. Both cantilever response time and oscillation amplitude reading time will decrease with an increase in cantilever resonant frequency[4], and it can also lead up to a lower Brownian vibration noise[4] limit. On the other hand, a low spring constant must be satisfied for biological application, since living cell membranes are extremely soft.

The resonant frequency of a multiple layer cantilever[7] equation is given

$$f_n = \frac{(k_n l)^2}{2\pi l^2}\left(\frac{\int_h E(z-z_0)^2 dz}{\sum_{i=1}^{N}(h_i \rho_i)}\right)^{1/2} \quad (3)$$

where E, l, h_i and ρ_i are the Young's Modulus of elasticity, length, thickness and densities of each layers, respectively. z_0 is the position of the neutral axis, k_n is a modal parameter, and $k_n l \approx 1.8751$ for first order mode.

The rectangular cantilever spring constant can be calculated by following equation[8].

$$k_c = \frac{wd^3}{4l^3}E \quad (4)$$

where d, w, l and E are the thickness, width, length and Young's modulus of the cantilever, respectively.

Since the entire cantilever can be regarded as composed of two cantilever beams with one having PZT layer and the other without connected in series, , the equivalent spring constant (k) obeys a law:

$$k = \frac{k_1 k_2}{k_1 + k_2} \quad (5)$$

where k_1 is the spring constant for the portion of the cantilever with PZT, and k_2 is the spring constant for the portion cantilever without PZT.

Considering the equation (5), if $k_1 \ll k_2$, the equivalent spring constant will be determined by k_2. Since k_2 is the spring constant of a silicon cantilever, which is very small value, the short PZT layer will lead to a low spring constant for the entire cantilever.

Figure 6 and 7 show the resonant frequency and spring constant for three different lengths of cantilevers with various PZT length and fixed 0.25um thickness, respectively. Clearly the graph shows an optimal PZT length to achieve maximum resonant frequency for each cantilever length. In addition, increasing the length of cantilever will reduce the resonant frequency. On the other hand, the shorter PZT layer or the longer cantilever will lead to a smaller spring constant. However, if the cantilever is too long, the resonant frequency and effective deflection range will be compromised. If the cantilever is too short, the PZT layer have to be long enough to achieve a desired displacement, which will cause a large spring constant. Thus a 12um cantilever beam with 0.25um thick and 6um long PZT layer is a relatively good compromise, as this structure has a 6.25MHz resonant frequency in air with a 0.195N/m spring constant. The minimum, maximum z-displacement and the displacement range are 49.1nm, 234.7nm and 185.6nm, respectively, for this cantilever.

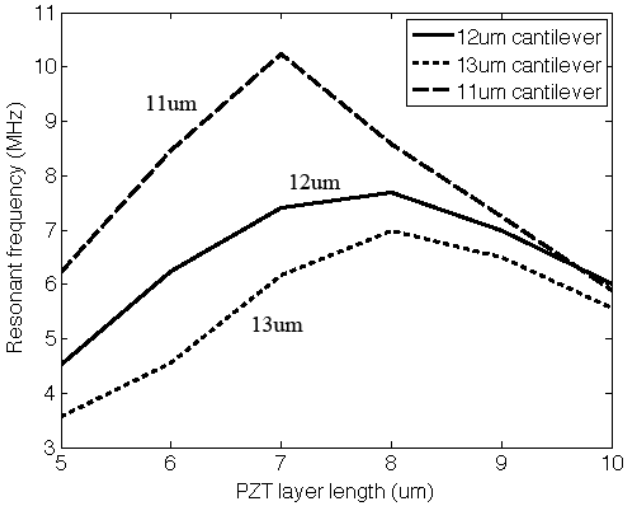

Figure 6. Resonant frequency for three cantilevers with different PZT layer dimension.

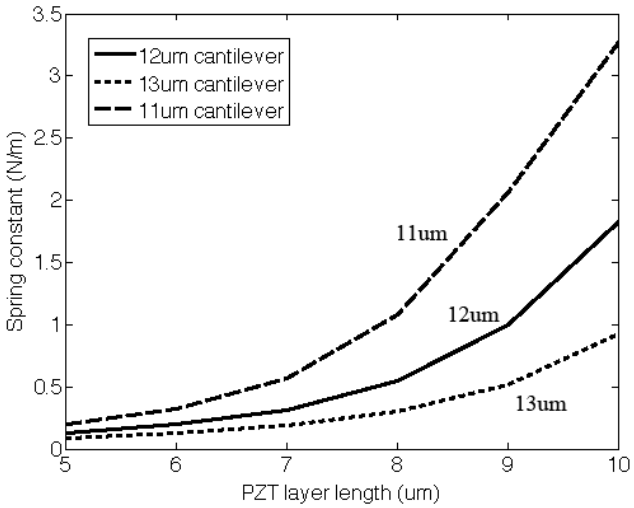

Figure 7. Spring constant for three cantilevers with different PZT layer dimension.

4. CONCLUSION

In this report, a theory and simulation studies on a new on-chip optical nano-scale displacement sensor for application in high-speed miniaturized AFM have been presented. The sensor consists of input and output cantilevered silicon waveguides separated by a small air-gap. An optical signal is coupled to the input waveguide and detected at the output waveguide. The out-of-plane deflection is measured from the change in the received power. A piezo-electric thin film actuator is integrated onto the cantilevered input silicon waveguide to allow a self-actuating feature for z-scanning. Theoretical, FDTD optical simulations, and ANSYS multi-physics simulations have been performed to study the sensor behavior. The results show that with an input silicon waveguide cantilever of 12μm long, 200nm wide, and 180nm thick with piezo-electric layer of 7μm long and 0.25μm thick, a sensitivity of less than 0.1nm, bandwidth of 6.25MHz in air and 0.195N/m spring constant has been achieved. The result is promising as it leads to high speed self-sensing and actuating cantilever that enables not only a high speed AFM but also large area scanning through parallel imaging.

REFERENCE

[1] Binnig, G., Quate, C. F., Gerber, Ch., "Atomic force microscope," Phys. Rev. Lett. 56, 930–933 (1986).

[2] Marti, O., Drake, B., Hansma, P. K., "Atomic force microscopy of liquid-covered surfaces: atomic resolution images," Appl. Phys. Lett. 51, 484–486 (1987).

[3] Parot, P., Dufreˆne, Y. F., Hinterdorfer, P., Grimellec, C. Le., Navajas, D., Pellequer, J. –L. and Scheuring, S., "Past, present and future of atomic force microscopy in life sciences and medicine," J. Mol. Recognit. 20, 418–431 (2007).

[4] Ando, T., "Video imaging of bimolecular processes by high-speed AFM". IEEE MEMS conference 24th, 57-62 (2011).

[5] Senior, J. M., [Optical Fiber Communication Principles and Practice], Pearson Education, Third edition, 610-611, 230-232, (2009).

[6] Shkuratov, S. I., Talantsev E. F. and Baird, J., "Electric breakdown of longitudinally shocked Pb(Zr0.52Ti0.48)O3 ceramics", J. Appl. Phys, 110, 024113 (2011).

[7] Sandberg, R., Svendsen, W., Molhave, K. and Boisen, A., "Temperature and pressure dependence of resonance in multi-layer microcantilevers" J. Micromech. Microeng. 15, 1454–1458 (2005).

[8] Poggi, M. A., McFarland, A. W. and Colton, J. S., "A Method for Calculating the Spring Constant of Atomic Force Microscopy Cantilevers with a Nonrectangular Cross Section", Anal. Chem. 77, 1192-1195 (2005).